

Magnetohydrodynamic Instability with Neutral-Beam Heating in the ISX-B Tokamak

J. L. Dunlap, B. A. Carreras, V. K. Paré, J. A. Holmes,^(a) S. C. Bates, J. D. Bell,^(a)

H. R. Hicks,^(b) V. E. Lynch,^(a) and A. P. Navarro^(b)

Oak Ridge National Laboratory, Oak Ridge, Tennessee 37830

(Received 16 October 1981)

This paper describes observations of magnetohydrodynamic instability with neutral-beam heating in the ISX-B tokamak and the theory specifically developed to support these experiments. The observed magnetohydrodynamic activity is explained by the resistive model presented but is not responsible for the observed degradation of confinement. Increasingly important $n > 1$ pressure-driven modes are predicted by the theory for the higher experimental β_p values, but there is no experimental verification of their presence.

PACS numbers: 52.55.Gb, 52.30.+r, 52.35.Py

The ISX-B tokamak operates with up to 2.5-MW auxiliary heating power (total) from two coinjected neutral beams. Confinement degrades with increasing beam power (P_b), and the quantity $\beta_p \sqrt{I_p}$ "saturates" as a function of P_b , where β_p denotes the volume-averaged poloidal β and I_p denotes the discharge current. Maximum volume-averaged total β obtained to date is $\approx 2.5\%$, well below values expected by extrapolation from results at low P_b . Descriptions of the device and of most other features of the neutral-beam experiments are available elsewhere.¹⁻⁴

Our observations of magnetohydrodynamic (MHD) instability have covered the wide range of plasma parameters involved in these neutral-beam experiments. In this Letter, we describe these observations and the theory specifically developed to support these high- β experiments. We arrive at mode identification and consider the role of this instability in the degradation of confinement. These issues are important because tokamak operation has only recently reached plasma regimes with such β values, and the limitation observed here causes concern about the viability of the tokamak as a reactor concept.

Mirnov coils and collimated soft-x-ray detectors were used for instability diagnostics. The coils were arranged in arrays to determine the dominant poloidal and toroidal mode numbers (m, n) of the poloidal field fluctuations \tilde{B}_p in the shadow of limiters. The x-ray studies mainly used detectors in a 32-unit fan array centered on the outside equatorial and in a 24-unit fan array centered on the top vertical center line in the same poloidal section. Even during operation with maximum bandwidths (≈ 125 kHz), instability signals from all diagnostic channels were dominated by frequencies in the 5- to 25-kHz range. Data acquisition was both oscillographic and digital, the

latter by a 56-channel CAMAC system.

Ohmically heated (OH) discharges suitable for injection heating in ISX-B are sawtoothing ones.⁵ Very low beam powers affect instability only by enhancing the amplitude and period of this classic sawtooth behavior. The instability signals are altered when the ratio of P_b to Ohmic power P_{OH} exceeds ≈ 1 . The changes are first marked by a longer interval of $m = 1$ activity before internal disruption and the simultaneous appearance of strong \tilde{B}_p at the same frequency as the $m = 1$. Thereafter, the envelopes of \tilde{X} and \tilde{B}_p , where \tilde{X} is the fluctuating level of the x-ray signal, vary with plasma parameters. Generally, further increases in beam power lead first to longer-lived, even steadily running precursors and then to increasing amplitude modulation of these signals. Under some conditions the appearance of a long-period sawtooth is retained; in other cases it is not. This description strictly applies only to edge $q_\psi \leq 4.5$, since patterns revert toward those of the classic sawtooth as q_ψ is increased.

Despite the variation of signal patterns with plasma parameters, the basic features of these signals do not change once the threshold $P_b/P_{OH} \approx 1$ is passed. The \tilde{B}_p at the Mirnov coils is strong, often exceeding $\tilde{B}_p/B_p = 1\%$ at major radius $R \approx R_0 + 0.3$ m near the outside equatorial, where ($m = 2; n = 1$) mode symmetry is dominant. From \tilde{B}_p , mode rotation is the reverse of that in OH plasmas, possibly because of toroidal rotation driven by the coinjected neutral beams.⁶ The large \tilde{X} signals are from within $q \approx 1$ and are due to a large $m = 1$ mode there. Rotation of this $m = 1$ structure is also reversed. Despite the large ($m = 2$)/($n = 1$) \tilde{B}_p , there is no large or distinctive \tilde{X} from near $q = 2$ and thus there can be only a small 2/1 island structure. The \tilde{X} wave forms show significant differences of detail when com-

pared with the work of others⁷ on the classic $m=1$.

The JFT-2 tokamak yields somewhat similar instability signals when operated with neutral-beam heating at β values like those of ISX-B.⁸ Not enough details from JFT-2 are available for a definite conclusion, but it appears that the same basic instability is present in both devices.

The stability properties of ISX-B-like plasmas have been studied in the framework of the resistive MHD model,⁹ a nonlinear, three-dimensional model expressed by a reduced set of resistive MHD equations valid in the limits of large aspect ratio ($\epsilon = a/R \ll 1$) and high β ($\beta \sim \epsilon$).¹⁰ The equilibria were obtained by solving the Grad-Shafranov equation (exact to all orders in ϵ) in a flux-conserving manner. For systematic theoretical studies, the equilibria were characterized by a pressure profile $p = p_0 \psi^2$, a safety factor (q) profile, and the shape of the outermost flux surface. Several sequences of equilibria were studied.⁹ They gave the same qualitative results. At low β_p , the most unstable mode is the $n=1$. Its linear stability properties with increasing β_p are summarized in Fig. 1. At low β and in the cylindrical limit, this mode is just the $(m=1; n=1)$ tearing mode. With increasing pressure, the mode goes from the tearing branch to a pressure-driven branch. Higher- n modes became linearly unstable with increasing β_p ; they are essentially pressure driven and have ballooning character.¹¹ All of these results are for equilibria stable to ideal modes.

For the lower range of β_p values obtained with

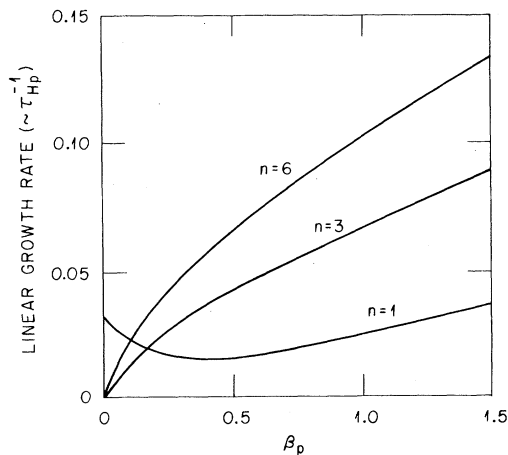


FIG. 1. Linear growth rates for $n=1$, $n=3$, and $n=6$ for circular cross-section plasma and q profile $q(\rho) = 0.9[1 + (\rho/0.65)^4]^{1/2}$, $0 \leq \rho \leq 1$.

beam heating in ISX-B ($\beta_p < 1$), the theory shows an instability that is best described as a β_p distortion of the $(m=1; n=1)$ mode. This mode drives many other helicities through the toroidal and nonlinear couplings. The main results are as follows: (1) For a given q profile, growth of the $m=1$ island slows down with increasing β_p , from exponential to linear, before reconnection takes place. (2) If β_p is high enough, the island saturates without reconnection and therefore produces continuous $m=1$ mode activity. This happens when the $(m=1; n=1)$ mode is primarily driven by pressure. (3) The largest driven mode is the $(m=2; n=1)$. This component, like the other driven modes, is mainly localized near the $q=1$ surface. It produces a large \tilde{B}_p at the limiter but only small $2/1$ islands near $q=2$ and hence only small \tilde{X} . (4) A broad spectrum of other driven modes is produced. These generate a variety of magnetic islands that often overlap and break magnetic surfaces (Fig. 2). (5) As the edge q is raised, the instability reverts toward the classical low- β $m=1$.¹² Growth of the $m=1$ island speeds up as a result of increasing shear at the $q=1$ surface, and the amplitudes of the driven modes and \tilde{B}_p at the limiter decrease because the radius of the $q=1$ is reduced.

These theoretical results and the gross features of the experimental observations are clearly in agreement. A comparison at a more detailed level is done by using equilibria reconstructed from laser-profile and magnetic data and calculating \tilde{X} wave forms from the theoretically predicted mode structure. In this procedure, \tilde{X} along vari-

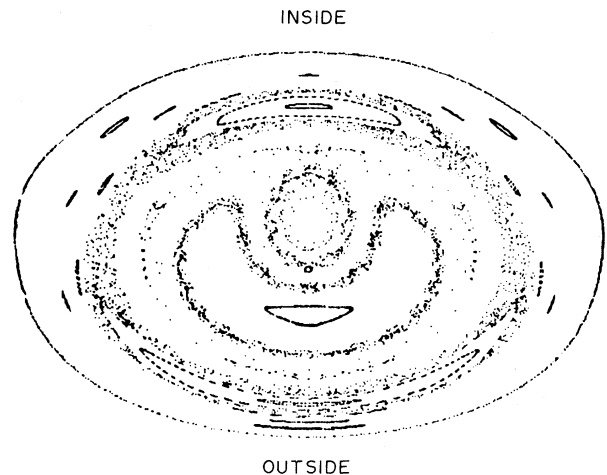


FIG. 2. Calculated field structure; a "snapshot" just before reconnection takes place.

ous chords was calculated as a line integral of p^2 , and toroidal rotation of the mode structure at a constant frequency ω was assumed. Figure 3 is a comparison of experimental and theoretically derived wave forms for the side-mounted array. The theoretical ones resulted from corotation of the instability structure shown in Fig. 2. Features of a dominant $m=1$ (Ref. 7) are evident in both displays. Additional fine-grained details are common to both: (1) The channel nearest center shows the expected dominant 2ω resulting from the $m=1$. Successive peaks on center are not of equal amplitude, a feature that in the model calculation results from the presence of the driven $m=2$ rotating in phase with the $m=1$. (2) The double humps on positive half cycles at nearby channels, e.g., 15 and 17, are also not equal and the ordering of the inequality reverses between upper and lower channels. These features are again the result of the $m=1$ and $m=2$ coupling. If counterrotation is assumed in the model, the theoretical traces for channels 15 and 17 are exchanged and then disagree with the experimental traces. (3) At channels 10 and 22, the wave forms are triangular in nature and are again reversed between upper and lower channels. This is just outside $q=1$, where the $(n=1; n=1)$ eigenfunction no longer dominates and so no longer ob-

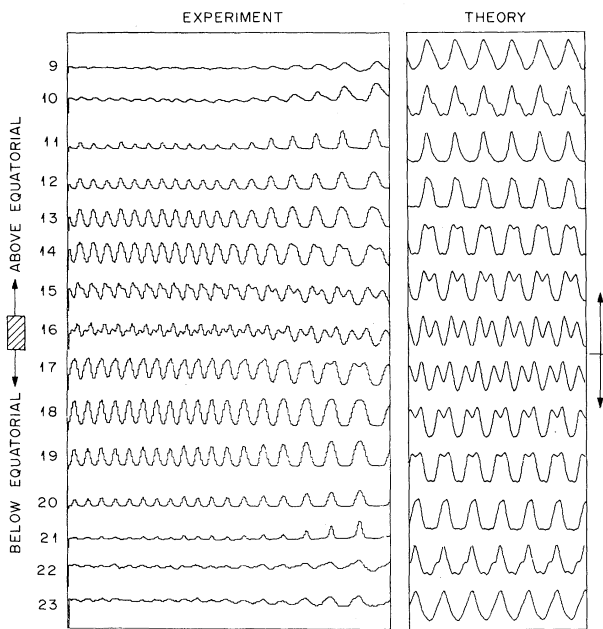


FIG. 3. Side-array wave forms, from 242 to 243.33 ms in the experiment. Viewing radii of the detectors, referenced to plasma center, step in equal increments from $r \approx 0$ to $r \approx 0.15$ m.

scures the effects of coherent superposition of all the other driven mode components. The assumption of counterrotation exchanges the theoretical traces and again leads to disagreement with the experimental ones.

As β_p increases to the higher ranges obtained in ISX-B, the role of additional $n > 1$ modes in the overall predicted mode structure becomes increasingly important. Since these modes are linearly unstable, they are not linked to the evolution of the $(n=1; n=1)$. At very low resistivity, these $n > 1$ modes saturate at small amplitude, but their overall level is large enough to potentially influence transport. At these values of resistivity and β_p , the numerical calculations are very difficult and their study is not yet complete.

In this higher- β_p regime, the experimental \tilde{B}_p and \tilde{X} wave forms continue to show the distorted $(n=1; n=1)$ mode. They have not shown the presence of the additional incoherent $n > 1$, high- β_p modes predicted by the theory. Because our diagnostics are signal-averaging in nature and may be restricted to too low frequencies, they may be insensitive to such highly structured modes.

We have no positive experimental correlation between observed mode activity and the degradation of confinement with increasing P_b . Our best efforts have been toroidal field (B_T) scans at fixed plasma current and density, which use the fact that raising edge q reduces the intensity of the $m=1$ and driven modes and, presumably, any associated losses. Scans at $P_b \approx 2$ MW yielded

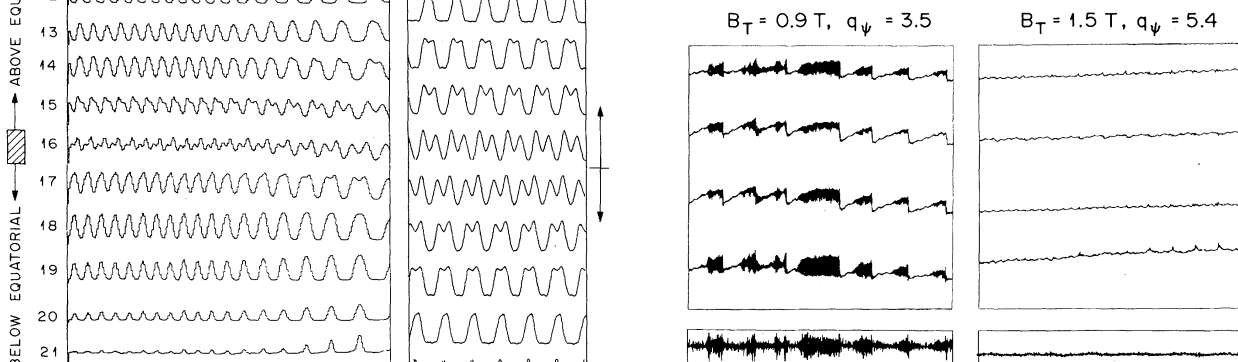


FIG. 4. Instability signals (upper curves: \tilde{X} from four central x-ray detectors; lower curves: \tilde{B}_p from near the outside equatorial) for two tokamak discharges. Left-hand side at low- B_T point and right-hand side at high- B_T point of the B_T scan. 160 to 208 ms in each discharge. Circular discharges ($\kappa \approx 1.2$), $\bar{n}_e = (6-7) \times 10^{13} \text{ cm}^{-3}$, $I_p = 140 \text{ kA}$.

essentially constant β_p despite marked changes in MHD intensity. With P_b reduced to 0.6 MW to produce a β_p value out of saturation and a plasma regime in which the independently unstable, high- n , pressure-driven modes are less likely to be important, the amplitude of the instability signals again decreased markedly as B_T was raised (Fig. 4). However, β_p did not increase; neither did the stored energy ($\propto \beta_p I_p^2$) or the gross confinement time ($\propto \beta_p I_p^2 / P_{in}$).

We conclude that the MHD activity observed in ISX-B is well understood in terms of the resistive MHD model and that this observed activity is not responsible for pronounced degradation of confinement. The $n > 1$, pressure-driven modes predicted by the model are a possible explanation for the observed degradation, but their presence in this plasma has not been experimentally verified.

We acknowledge with appreciation the support of our many colleagues in the ISX-B group and in the engineering staff. This research was sponsored by the Office of Fusion Energy, U. S. Department of Energy, under Contract No. W-7405-eng-26 with the Union Carbide Corporation.

^(a)On assignment from Nuclear Division, Computer Sciences, Union Carbide Corporation, Oak Ridge,

Tenn. 37830.

^(b)Present address: Junta de Energía Nuclear, Madrid, Spain.

¹M. J. Saltmarsh, *J. Vac. Sci. Technol.* **17**, 260 (1980).

²M. Murakami *et al.*, in *Plasma Physics and Controlled Nuclear Fusion Research—1980* (International Atomic Energy Agency, Vienna, 1981), Vol. I, p. 377.

³D. W. Swain *et al.*, "High Beta Injection Experiments on the ISX-B Tokamak," to be published.

⁴E. A. Lazarus *et al.*, in *Proceedings of the Tenth European Conference on Controlled Fusion and Plasma Physics*, Moscow, 14–19 September 1981 (to be published).

⁵S. von Goeler, W. Stodiek, and N. R. Sauthoff, *Phys. Rev. Lett.* **33**, 1201 (1974).

⁶S. Suckewer, H. P. Eubank, R. J. Goldston, E. Hinov, and N. R. Sauthoff, *Phys. Rev. Lett.* **43**, 207 (1979).

⁷N. R. Sauthoff, S. von Goeler, D. R. Eames, and W. Stodiek, in *Proceedings of the International Atomic Energy Agency Symposium on Current Disruption in Toroidal Devices*, Max-Planck-Institut für Plasmaphysik Report No. IPP 3/51, 1979 (unpublished), paper C-5.

⁸S. Yamamoto *et al.*, *Nucl. Fusion* **21**, 993 (1981).

⁹J. A. Holmes *et al.*, Oak Ridge National Laboratory Report No. ORNL/TM-8063, 1982 (unpublished).

¹⁰H. R. Strauss, *Phys. Fluids* **20**, 1354 (1977).

¹¹H. R. Hick *et al.*, in *Plasma Physics and Controlled Nuclear Fusion Research—1980* (International Atomic Energy Agency, Vienna, 1981), Vol. I, p. 259.

¹²G. L. Jahns *et al.*, *Nucl. Fusion* **18**, 609 (1978).

Density-Wave Theory of First-Order Freezing in Two Dimensions

T. V. Ramakrishnan^(a)

Bell Laboratories, Murray Hill, New Jersey 07974

(Received 9 November 1981)

The spontaneous formation of a finite-amplitude density wave of hcp lattice symmetry is discussed, following the work of Ramakrishnan and Yussouff. The freezing parameters do not depend on the interatomic force law, contain no adjustable parameters, and can be improved perturbatively. The results agree very well with those from computer simulation for a wide range of systems.

PACS number: 64.70.Dv

There has been considerable recent interest in the nature of the liquid-solid transition in two dimensions,¹ spurred by the development of a beautiful and detailed dislocation unbinding theory due to Halperin and Nelson² (and also Young²) based on the ideas of Kosterlitz and Thouless.³ Many experiments and computer experiments have been carried out^{1,4} to test its novel predictions, e.g., that there is a hexatic phase be-

tween the solid and the isotropic liquid, and that the transitions are thermodynamically continuous. Most recent computer simulations, e.g., on the Lennard-Jones system at constant pressure,⁵ and r^{-n} systems with $n = 12$,^{6,7} $n = 3$,^{8,9} and $n = 1$,¹⁰ show a first-order transition and no hexatic phase. Freezing parameters such as the entropy change $(\Delta S/k_B)^{6-10}$ and the structure factor peak near freezing^{7,9,11,12} are close to 0.3 and 5.0, re-